

Multi-view Improved Monitored Distillation for Depth Completion

Jia-Wei Guo¹, Cong Li¹, Sen-Hua Zhu², Chang-Zheng Zhang², Ming Ouyang², Ning Ding³,
Hung-Chyun Chou¹

Abstract—This paper proposes a new depth completion method based on multi-view improved monitored distillation to generate more accurate depth maps. Based on the state-of-the-art depth completion method named ensemble distillation, we introduce an existing stereo-based model as a teacher model to improve ensemble distillation accuracy and generate a more accurate student model in training by avoiding inherent error modes of completion-based teachers as well as minimizing the reconstruction error for a given image. We also leverage multi-view depth consistency and multi-scale minimum reprojection to provide self-supervised information. These methods use the existing structure constraints to yield supervised signals for student model training without great expense on gathering ground truth information of depth. Our extensive experimental evaluation demonstrates that our proposed method can effectively improve the accuracy of baseline method of monitored distillation.

I. INTRODUCTION

Scene depth perception has been used in many fields, such as automatic driving, robotics, augment-reality, and so forth [1, 2, 3]. Scene depth information can be obtained using LiDAR, RGB-D and stereo cameras [1, 4, 5]. But these sensors have disadvantages, such as high costs, limited measure distance and high-power consumption. In recent years, more research has focused on learning-based depth estimation and yielded many efficient and high-accuracy technologies [4, 6, 7]. Depth completion is one of the most popular research directions among deep learning applications, aiming to estimate dense pixel-wise depth from an extremely sparse map obtained by a depth sensor [8, 9].

Deep learning-based methods for depth completion have shown remarkable performance on the task and led a development trend. In prior works, missing depths can be completed using a network with several convolutional layers [10] or a simple auto-encoder [11] with a dataset of images and corresponding sparse depths. The traditional method of this type is to exploit dual encoders for extracting detailed features from an RGB image and its corresponding sparse depth map and then fuse them using a decoder [12, 13]. For

depth completion, recent research tends to use complicated network frameworks and learning strategies. Apart from feature fusion from image and sparse depth, researchers have begun to introduce surface normal [14], affinity matrix [15], residual depth map [16] and so forth into their methodologies. Besides, to deal with the lack of supervised pixels, some research focused on knowledge distillation [17], multi-view geometric constraints [18, 19] and adversarial regularization [20]. In [21], a blind ensemble distillation of teacher models was exploited to yield a distilled depth map with minimum reconstruction error and a confidence map. These maps can be used to train more accurate student models by selectively learning the best pixel-wise depth estimation from the ensemble and avoiding learning the teachers' error modes.

When the procedure of assembling teachers' results yields high photometric reprojection errors, the student can only rely on unsupervised losses to obtain the correct model parameters. To solve this problem, we introduce a novel stereo-based teacher to generate supervised signals as a constraint for student training. Also, we exploit multi-view depth consistency between time-sequential to promote the convergence of student model training further. The training can be fined by using multi-scale minimum reprojection among decoder layers. Our extensive experiments on benchmark datasets KITTI demonstrate the effectiveness of the proposed method. Compared to the state-of-the-art depth completion methods on KITTI, our improved distillation method outperforms those across generous four metrics.

II. RELATED WORKS

A. Learning-Based Stereo Estimation

Most stereo estimation algorithms infer scene depth information by computing the similarity between each pixel in the left image and the corresponding pixel in the right image. Generally calibrated stereo image pair is used for input, so the disparity estimation, i.e., scaled inverse depth, can be conducted as a 1-D search. A typical learning-based stereo estimation consists of four steps: matching cost computation, cost aggregation, optimization, and disparity refinement.

Traditional studies focus on computing the matching cost using convolution layers and applying semi-global matching (SGM) to refine the disparity result [22]. Recently, end-to-end networks have been developed to predict whole disparity results without an explicit feature-matching module or post-processing [23, 24]. PSM-Net [25] proposed an end-to-end learning framework for stereo matching without post-processing. And a pyramid pooling module was introduced into image features, which further incorporates global context information to improve feature extraction accuracy. In this paper, we leverage a stereo-based learning

*This work was supported by National Key R&D Program of China No. U2013202 and the Guangdong Basic and Applied Basic Research Foundation under Grant No. 2022A1515011139. Corresponding author: Hung-Chyun Chou, Email: zhouhongjun@cuhk.edu.cn

Authors 1 are with Special Robot Center, Shenzhen Institute of Artificial Intelligence and Robotics for Society, 14-15F, Tower G2, Xinghe World, Rd Yabao, Longgang District, Shenzhen, Guangdong, 518129, China.

Authors 2 are with Huawei Cloud Computing Technology Co., Ltd.

Author 3 is with Shenzhen Institute of Artificial Intelligence and Robotics for Society, and Institute of Robotics and Intelligent Manufacturing, The Chinese University of Hong Kong, Shenzhen, Shenzhen, Guangdong, 518172, China.

model to further enhance the accuracy of supervised information during monitored knowledge distillation.

B. Unsupervised Depth Completion

Typical supervised depth completion methods require ground truth information as supervised signals for model training, which is hard to realize. While unsupervised depth completion methods can use inherent structure cues relating to the pose between adjacent images to improve model accuracy during training. Most of them focus on designing losses that minimize the photometric error between input images and other images reconstructed from different views or the difference between the estimation and sparse depth [12, 18, 19]. Other researchers used synthetic data to learn priors on the shapes populating a scene [26, 27]. And the efficiency of structure information plays a crucial role in the completion result of model training. We introduce multi-view depth consistency to supervise model training for better depth completion accuracy and simultaneously improve structure information accuracy during training.

C. Knowledge Distillation

Knowledge distillation aims to use a simpler student model to learn the function from a larger, more complicated teacher model by teacher's supervision. In recent work, some researchers have exploited this method to conduct depth estimation and have obtained effective results [28, 29]. [1] used cycle inconsistency and knowledge distillation for unsupervised monocular depth estimation, where the student network is part of teacher network. [21] leveraged ensemble learning to adaptively select the best pixel-wise depth result from each teacher model and avoid learning error modes from these models. Inspired by [18, 21], we introduce multi-scale minimum reprojection to further improve the accuracy of monitored distillation for depth completion without additional inputs.

III. PROPOSED METHOD

A. Overview

This work aims to obtain the dense depth of a scene from a single image and its corresponding sparse depth map. We propose a depth completion function that inputs RGB image I_t , its sparse depth z_t , and its corresponding camera intrinsics K_t and outputs a dense depth map d_t .

$$d_t := f_{\theta}(I_t, z_t, K_t) \in \mathbb{R}^{H \times W} \quad (1)$$

During training time, we consider that a set of synchronized pairs of images and sparse depth maps $\{I_i, z_i\}$, $I \in [t-1, t, t+1]$ is available, which is temporally adjacent. Also we have access to the corresponding image I_r of image I_t , which can be used for stereo-based depth estimation. Besides, we assume a set of N teacher depth outputs $\{d_h^i\}$, $i \in N$ related to image I_t is available from publicly pretrained models. In training, we input synchronized image-SD (sparse depth) pairs into student model, and it outputs a set of depth outputs $\{d_i\}$, $i \in [t-1, t, t+1]$ by depth completion function as (1). Meanwhile, we generate reconstructed images I_r' corresponding to I_t based on image warping function

$$I_r' = f_{\omega}(I_t, d_h) \quad (2)$$

The reconstructed I_r' can be used to generate the error map E by comparing to I_t based on the photometric reprojection error. Then, the error can be used to validate the correctness of teacher outputs $\{d_h\}$. From the error, we can construct distilled depth d_d by selecting the best pixel-wise values with the highest confidence from $\{d_h\}$ adaptively. After that, we use stereo outputs d_s from stereo-based depth model estimation to update the distilled depth by comparing the confidence of depth values.

During training, we introduce multi-view depth consistency (d_{t-1}, d_t, d_{t+1}) to supervise student model training for better accuracies of depth completion and structure information simultaneously. Then, we introduce multi-scale minimum reprojection to further improve the accuracy of monitored distillation for depth completion without additional inputs.

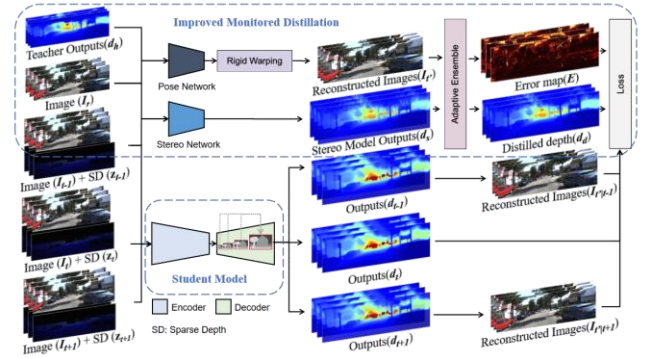


Fig.1. The framework of proposed monitored distillation

B. Stereo Constraint Supervision

In the module of monitored distillation, we use depth completion models as teacher for depth distillation [21]. To improve the accuracy of distilled depth in knowledge distillation, a stereo-based end-to-end depth estimation model [25] generates dense depth output d_s by giving a pair of left-right RGB images and producing a disparity map D that minimizes a matching cost function in (3).

$$E(D) = \sum C(x, d_x) \quad (3)$$

Here, $C(x, d_x)$ represents the cost of matching the pixel $x = (i, j)$ of the left image with the corresponding pixel $y = (i, j - d_x)$ in the right image. Due to unique feature extraction and fusion using the rich texture information in left-right images, a stereo-based depth estimation method can yield more accurate depth values in scene detail than a depth completion method. As shown in Fig. 2, the depth output from a stereo-based method is smoother than the result from the depth completion method. Therefore, we use stereo outputs d_s from stereo-based depth model estimation to update the distilled depth through comparing the confidence of depth values.

$$d_d^j = d_s^i \text{ if } E_d^j < E_s^i \quad (4)$$

We leverage stereo-based information as supervised information to further improve the accuracy of distilled depth d_d during monitored knowledge distillation.

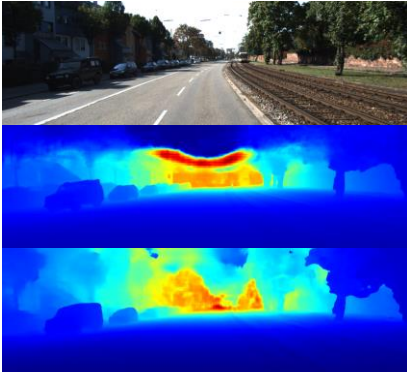


Fig. 2. Depth output from depth completion method (middle) and stereo-based method (bottom)

C. Multi-view Depth Consistency

Most depth estimation methods don't consider the depth consistency between all adjacent views. During training, we input current images and their adjacent images into a student model. Then the student model outputs the corresponding depth outputs $\{d_i\}$, $i \in [t-1, t, t+1]$. All depth outputs are used to reconstruct their corresponding adjacent views through the warping function. We construct photometric and structure loss functions to calculate the errors between all reconstructed adjacent images.

$$L_{\text{photometric}} = \sum(|\mathbf{I}_x - \mathbf{I}_x'|) \quad (5)$$

$$L_{\text{structure}} = \sum(1 - \psi(\mathbf{I}_x, \mathbf{I}_x')) \quad (6)$$

Here, $x, x', y \in [t-1, t, t+1]$, $x' \neq y$ and ψ represents structural similarity index distance, SSIM. Due to the fact of student network and pose network are responsible for the errors, the errors can be supervision information to supervise model training for better accuracy of depth completion especially when the monitored teacher distillation yields undesirable depth output with low confidence values [21]. And these losses can also simultaneously improve the accuracy of structure information during training.

D. Multi-scale Minimum Reprojection

Inspired by the methods of improvement on depth quality [18], we introduce multi-scale reprojection supervision into loss function during depth model training. Firstly, we upsample the lower resolution depth outputs (i.e. the intermediate outputs) to the input image resolution. Using (2), we then calculate the photometric error compared to other highest resolution views based on these upsampled depth outputs as shown in Fig. 3. This method is similar to matching patches, which means low-resolution disparity values will be responsible for reconstructing certain block of pixels in the highest resolution image directly. This can effectively supervise each scale resolution layer to converge toward the same direction that accurately reconstructs the highest resolution target image.

In order to reduce influence of occluded pixels causing high photometric error in multi-view feature matching, we introduce the minimum operation into photometric and structure loss over all adjacent images. The final per-pixel photometric and structure loss (7) and (8) are transferred from

(5) and (6).

$$L_{\text{photometric}} = \sum(\min_{\text{per-pixel}} |\mathbf{I}_x - \mathbf{I}_x'|) \quad (7)$$

$$L_{\text{structure}} = \sum(1 - \min_{\text{per-pixel}} (\psi(\mathbf{I}_x, \mathbf{I}_x')))) \quad (8)$$

IV. EXPERIMENTS

We evaluate our proposed method on publicly available benchmarks and compare its performance with previously published methods. All experiments are performed without ground truth for training.

A. Experimental Setup and Benchmark

We perform experiments on large-outdoor KITTI driving datasets. The datasets contain about 86,000 raw 1242x375 image frames and their corresponding synchronized sparse depth maps. These images are recorded from two video cameras and a LiDAR sensor, which valid area of sparse depth covers about 5% of the image space. We use the designated 1,000 samples and their corresponding ground truth depths with semi-dense data for validation.

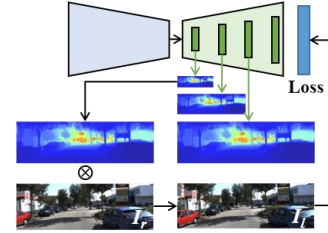


Fig. 3. Multi-scale photometric reprojection

For distillation models, We follow [21] to use PENet [30], MSG_CHN [31], ENet [30] and NLSPN [32] as depth completion teacher ensembles. And we introduce PSMNet [25] as a stereo-based depth estimation teacher for distillation improvement. Moreover, we perform the quantitative evaluation of our method according to several metrics used in previous works [21], as shown in Table 1. Let P be the total number of pixels in the test maps and \mathbf{d}_e , \mathbf{d}_{gt} represent the estimated depth and ground truth depth.

Table 1. Evaluation metrics.

Metric	Definition
MAE	$(\sum \mathbf{d}_e - \mathbf{d}_{gt}) / P$
RMSE	$(\sum \mathbf{d}_e - \mathbf{d}_{gt} ^2 / P)^{1/2}$
iMAE	$(\sum 1/\mathbf{d}_e - 1/\mathbf{d}_{gt}) / P$
iRMSE	$(\sum 1/\mathbf{d}_e - 1/\mathbf{d}_{gt} ^2 / P)^{1/2}$

B. Baselines for Ablation

To perform the ablation study presented in results, we use the following baselines.

Stereo-based learning: a stereo-based model will be introduced into the basic framework [21], and then the stereo outputs \mathbf{d}_s from stereo-based depth model estimation will be used to optimize the distilled depth \mathbf{d}_d .

Multi-view Depth Consistency: based on the basic framework, multi-view adjacent images and their corresponding sparse maps will be inputted into student model. And it outputs the corresponding depth outputs $\{d_i\}$, $i \in [t-1, t, t+1]$, which are used to construct photometric loss.

Multi-scale Minimum Reprojection: multi-scale reprojection supervision will be introduced into loss function during depth model training with the per-pixel minimum operation.

The proposed method: stereo-based learning (SL), multi-view depth consistency (MC) and multi-scale minimum reprojection (MR) will be performed simultaneously in the basic framework.

C. Results

In order to demonstrate the validity of our proposed method, we conduct an ablation study on the KITTI datasets. Results are shown in Table 2.

Table 2. Evaluation metrics

Method	MAE	RMSE	iMAE	iRMSE
Baseline	223.021	808.190	0.953	2.300
MR	224.588	816.997	0.943	2.269
MC	222.715	810.013	0.955	2.286
SL	222.177	806.855	0.949	2.280
Ours	221.897	807.063	0.952	2.270

In Table 2, we can note that our proposed sub-module methods have at least two items of metric better than the baseline method, which trained by KITTI datasets. And the method of introducing a stereo-based learning model has better values than the baseline in all four metrics. Our final method outperforms the baseline method across all metrics and effectively improve the depth maps as shown in qualitative comparisons on KITTI.

Table 3. Unsupervised method comparisons

Method	MAE	RMSE	iMAE	iRMSE
AdaFrame	291.620	1125.670	1.160	3.320
SynthProj	280.420	1095.260	1.190	3.530
ScaffNet	280.760	1121.930	1.150	3.300
KBNet	256.760	1069.470	1.020	2.950
Ours	221.897	807.063	0.952	2.270

In Table 3, we compare with several state-of-the-art works, considering both unsupervised learning-based, including AdaFrame, SynthProj, ScaffNet and KBNet, and supervised learning-based, such as SS-S2D, DeepLiDAR, ENet, PENet and NLSPN methods. As shown in Table 3, our method outperforms all the unsupervised learning-based method in all four metrics. And in Table 4 of supervised learning-based method, our method also achieves a great result among these methods, which better than SS-S2D and DeepLiDAR.

As shown in Fig. 4, our proposed method can improve the details of estimation depth maps comparing to baseline method, like car, pole, road lamp, etc.

Table 4. Supervised method comparisons

Method	MAE	RMSE	iMAE	iRMSE
SS-S2D	249.950	814.730	1.210	2.800
DeepLidar	226.500	758.380	1.150	2.560
Ours	221.897	807.063	0.952	2.270
ENet	216.260	741.300	0.950	2.140
PENet	210.550	730.080	0.940	2.170
NLSPN	199.590	741.680	0.840	1.990

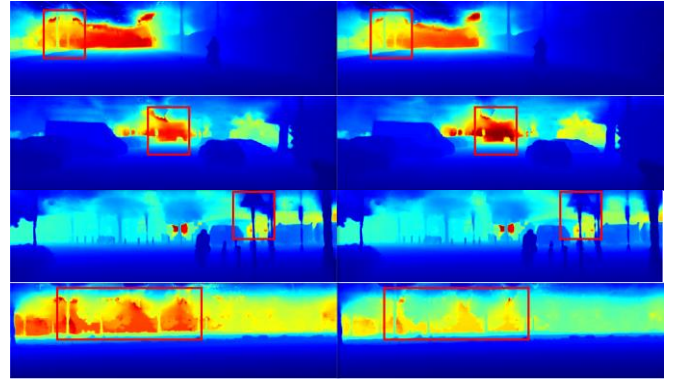


Fig. 3. Qualitative comparisons (LHS: the proposed method, RHS: baseline).

V. CONCLUSION

A new depth completion method based on multi-view improved monitored distillation is proposed in the paper, which generate more accurate depth map. We introduce a publicly stereo-based model as teacher model to improve ensemble distillation accuracy. We also leverage multi-view depth consistency and multi-scale minimum reprojection to provide self-supervised information, which further improve the accuracy of depth maps. These methods take advantage of the existing structure constraints to yield supervised signals for student model training without expense ground truth information. Our extensive experimental evaluation demonstrate that our proposed method can effectively improve the accuracy of baseline method of monitored distillation with MAE down to 221.897 from 223.021, RMSE down to 807.063 from 808.190, iMAE down to 0.952 from 0.953, iRMSE down to 2.270 from 2.300. The disadvantage of method is that can't handle some scene, like high reflective, rapidly light changing, transparent object and so forth, which can be further researched in the future.

REFERENCES

- [1] Z. Song, J. Lu, Y. Yao, and J. Zhang, "Self-supervised depth completion from direct visual-LiDAR odometry in autonomous driving," *IEEE Trans. Intelligent Transportation Systems*, vol. 23, no. 8, pp. 11654-11665, 2021.
- [2] F. Ma, L. Carlone, U. Ayaz, and D. Karaman, "Sparse depth sensing for resource-constrained robots," *Int. J. Robotics Research*, vol. 38, no. 8, pp. 935-980, 2019.

- [3] R. Du, E. Turner, M. Dzitsiuk, L. Prasso, I. Duarte, J. Dourgarian, and D. Kim, "DepthLab: Real-time 3D interaction with depth maps for mobile augmented reality," in *Proc. 33rd Annual ACM Symposium on User Interface Software and Technology*, 2020, pp. 829-843.
- [4] H. Laga, L. V. Jospin, F. Boussaid, and M. Bannamoun, "A survey on deep learning techniques for stereo-based depth estimation," *IEEE Trans. Pattern Analysis and Machine Intelligence*, vol. 44, no. 4, pp. 1738-1764, 2020.
- [5] N. Silberman, D. Hoiem, P. Kohli, and R. Fergus, "Indoor segmentation and support inference from rgbd images," in *Proc. Eur. Conf. Computer Vision (ECCV)*, 2012, pp. 746-760.
- [6] F. Tian, Y. Gao, Z. Fang, Y. Fang, J. Gu, H. Fujita, and J. N. Hwang, "Depth estimation using a self-supervised network based on cross-layer feature fusion and the quadtree constraint," *IEEE Trans. Circuits and Systems for Video Technology*, vol. 32, no. 4, pp. 1751-1766, 2021.
- [7] J. Hu, C. Bao, M. Ozay, C. Fan, Q. Gao, H. Liu, and T. L. Lam, "Deep Depth Completion from Extremely Sparse Data: A Survey," *IEEE Trans. Pattern Analysis and Machine Intelligence*, 2022.
- [8] Z. Huang, J. Fan, S. Cheng, S. Yi, X. Wang, and H. Li, "Hms-net: Hierarchical multi-scale sparsity-invariant network for sparse depth completion," *IEEE Trans. Image Processing*, vol. 29, pp. 3429-3441, 2019.
- [9] J. Liu, X. Gong, and J. Lin, "Guided inpainting and filtering for kinect depth maps," in *Proc. 21st International Conference on Pattern Recognition (ICPR)*, 2012, pp. 2055-2058.
- [10] J. Uhrig, N. Schneider, L. Schneider, U. Franke, T. Brox, and A. Geiger, "Sparsity invariant cnns," in *Proc. IEEE International Conference on 3D Vision (3DV)*, 2017, pp. 11-20.
- [11] K. Lu, N. Barnes, S. Anwar, and L. Zheng, "Depth completion auto-encoder," in *Proc. IEEE/CVF Winter Conference on Applications of Computer Vision Workshops (WACVW)*, 2022, pp. 63-73.
- [12] A. Wong, and S. Soatto, "Unsupervised depth completion with calibrated backprojection layers," in *Proc. IEEE/CVF Conference on Computer Vision and Pattern Recognition*, 2021, pp. 12747-12756.
- [13] S. S. Shivakumar, T. Nguyen, I. D. Miller, S. W. Chen, V. Kumar, and C. J. Taylor, "Dfusenet: Deep fusion of rgb and sparse depth information for image guided dense depth completion," in *Proc. IEEE Intelligent Transportation Systems Conference (ITSC)*, 2019, pp. 13-20.
- [14] J. Qiu, Z. Cui, Y. Zhang, X. Zhang, S. Liu, B. Zeng, and M. Pollefeys, "Deeplidar: Deep surface normal guided depth prediction for outdoor scene from sparse lidar data and single color image," in *Proc. IEEE/CVF Conference on Computer Vision and Pattern Recognition*, 2019, pp. 3313-3322.
- [15] X. Cheng, P. Wang, and R. Yang, "Depth estimation via affinity learned with convolutional spatial propagation network," in *Proc. Eur. Conf. Computer Vision (ECCV)*, 2018, pp. 103-119.
- [16] J. Gu, Z. Xiang, Y. Ye, and L. Wang, "DenseLiDAR: A real-time pseudo dense depth guided depth completion network," *IEEE Robotics and Automation Letters*, vol. 6, no. 2, pp. 1808-1815, 2021.
- [17] Pilzer, S. Lathuiliere, N. Sebe, and E. Ricci, "Refine and distill: Exploiting cycle-inconsistency and knowledge distillation for unsupervised monocular depth estimation," in *Proc. IEEE/CVF Conference on Computer Vision and Pattern Recognition*, 2019, pp. 9768-9777.
- [18] C. Godard, O. Mac Aodha, M. Firman, and G. J. Brostow, "Digging into self-supervised monocular depth estimation," in *Proc. IEEE International Conference on Computer Vision*, 2019, pp. 3828-3838.
- [19] C. Godard, O. Mac Aodha, and G. J. Brostow, "Unsupervised monocular depth estimation with left-right consistency," in *Proc. IEEE Conf. Computer Vision and Pattern Recognition (CVPR)*, 2017, pp. 270-279.
- [20] A. Pilzer, D. Xu, M. Puscas, E. Ricci, and N. Sebe, "Unsupervised adversarial depth estimation using cycled generative networks," in *Proc. IEEE International Conference on 3D Vision (3DV)*, 2018, pp. 587-595.
- [21] T. Y. Liu, P. Agrawal, A. Chen, B. W. Hong, and A. Wong, "Monitored distillation for positive congruent depth completion," in *Proc. Eur. Conf. Computer Vision (ECCV)*, 2022, pp. 35-53.
- [22] A. Shaked, and L. Wolf, "Improved stereo matching with constant highway networks and reflective confidence learning," in *Proc. IEEE Conf. Computer Vision and Pattern Recognition (CVPR)*, 2017, pp. 4641-4650.
- [23] A. Kendall, H. Martirosyan, S. Dasgupta, P. Henry, R. Kennedy, A. Bachrach, and A. Bry, "End-to-end learning of geometry and context for deep stereo regression," in *Proc. IEEE International Conference on Computer Vision*, 2017, pp. 66-75.
- [24] C. Won, J. Ryu, and J. Lim, "End-to-end learning for omnidirectional stereo matching with uncertainty prior," *IEEE Trans. Pattern Analysis and Machine Intelligence*, vol. 43, no. 11, pp. 3850-3862, 2020.
- [25] J. R. Chang, and Y. S. Chen, "Pyramid stereo matching network," in *Proc. IEEE Conf. Computer Vision and Pattern Recognition (CVPR)*, 2018, pp. 5410-5418.
- [26] A. Wong, X. Fei, S. Tsuei, and S. Soatto, "Unsupervised depth completion from visual inertial odometry," *IEEE Robotics and Automation Letters*, vol. 5, no. 2, pp. 1899-1906, 2020.
- [27] Y. Yang, A. Wong, and S. Soatto, "Dense depth posterior (ddp) from single image and sparse range," in *Proc. IEEE/CVF Conference on Computer Vision and Pattern Recognition*, 2019, pp. 3353-3362.
- [28] J. Hu, C. Fan, H. Jiang, X. Guo, Y. Guo, X. Lu, and T. L. Lam, "Boosting light-weight depth estimation via knowledge distillation," *arXiv preprint arXiv:2105.06143*, 2021.
- [29] Y. Liu, C. Shu, J. Wang, and C. Shen, "Structured knowledge distillation for dense prediction," *IEEE Trans. Pattern Analysis and Machine Intelligence*, 2020.
- [30] M. Hu, S. Wang, B. Li, S. Ning, L. Fan, and X. Gong, "Penet: Towards precise and efficient image guided depth completion," in *Proc. IEEE International Conference on Robot Automation (ICRA)*, 2021, pp. 13656-13662.
- [31] A. Li, Z. Yuan, Y. Ling, W. Chi, and C. Zhang, "A multi-scale guided cascade hourglass network for depth completion," in *Proc. IEEE/CVF Winter Conference on Applications of Computer Vision Workshops (WACVW)*, 2020, pp. 32-40.
- [32] J. Park, K. Joo, Z. Hu, C. K. Liu, and I. So Kweon, "Non-local spatial propagation network for depth completion," in *Proc. Eur. Conf. Computer Vision (ECCV)*, 2020, pp. 120-136.